

Effects of GaP Insertion Layer on the Properties of InP Nanostructures by Metal-Organic Vapor Phase Epitaxy

Soe Soe Han¹, Somsak Panyakeow², Somchai Ratanathamphan³,
Akio Higo⁴, Wang Yunpeng⁵, Momoko Deura⁵, Masakazu Sugiyama⁶,
Yoshiaki Nakano⁷

Abstract

The influence of thin GaP insertion layers (0 – 4) monolayers (MLs) on the properties of InP self-assembled quantum dots (SAQDs) embedded in $\text{In}_{0.49}\text{Ga}_{0.51}\text{P}$ matrix on GaAs (001) substrate grown by metal-organic vapor phase epitaxy was reported. In order to reduce the dots diameter and improve the size uniformity and photoluminescence (PL) emission, GaP layers thickness (0-4) monolayers (MLs) were inserted. The growth of thin GaP insertion layer (IL) between $\text{In}_{0.49}\text{Ga}_{0.51}\text{P}$ matrix and InP QDs layer reduced the mean height and size fluctuation and increased the density of InP QDs. The room-temperature (RT) PL emission could be observed around 780 nm red spectral range. The blue-shift of the PL peak was enhanced with thicker GaP insertion layer. The measurement of low-temperature (20 - 250 K) shows dependence of PL intensity on temperature.

Key words: InP, GaP, InGaP, Self-assembled Quantum Dots (SAQDs), Metal-Organic Vapor Phase Epitaxy (MOVPE)

Introduction

Self-assembled quantum dots (SAQDs) have been widely applied to semiconductor lasers, photo-detectors and quantum computation (Ribeiro E. et al., 2002). In the future, one can think of a simple QD device for using in computer or networking applications. For these purposes, optically or electrically addressable single QDs are needed on a mass production scale which favors metal-organic vapor-phase epitaxy (MOVPE)

-
1. Assistant Lecturer, Department of Physics, University of Yangon
 2. Professor, Department of Electrical Engineering, Chulalongkorn University
 3. Associate Professor, Department of Electrical Engineering, Chulalongkorn University
 4. Assistant Professor, Department of Information Devices, University of Tokyo
 5. Lecturer, Department of Electrical Engineering, University of Tokyo
 6. Associate Professor, Department of Electrical Engineering, University of Tokyo
 7. Professor, Department of Electrical Engineering, University of Tokyo

due to several advantages (DenBaars S.P. et al., 1994). By using InP QDs embedded in $\text{In}_{0.49}\text{Ga}_{0.51}\text{P}$ emission in this spectral range can be achieved (Richter. D. et al., 2010). In addition, InP QDs can be used to fabricate the shortest-wavelength laser structures emitting in the red spectral range. However, InP/InGaP SAQDs on GaAs are usually formed with poor size uniformity compared to that of InAs/GaAs QDs (Zwiller. V. et al., 2001). Especially, inhomogeneous broadening in optical spectra due to the randomness in the dot size has been a difficult issue of limiting potential benefits. While in the case MOVPE of InP/ InGaP SAQDs, a bimodal size distribution for the coherent islands has often been observed at low coverage of InP (Ren. H.-W. et al., 1997). This bimodal size distribution can be overcome by the insertion of GaP insertion layer (Leonard. D. et al., 1994). Nevertheless, the island size still remains large and hence the areal density is low (Thompson, A. G. et al., 1997). Since large dots may introduce misfit dislocations and low areal density of dots gives poor optoelectronic efficiency, growth of small size, high density and highly uniform InP/InGaP SAQDs becomes imperative (Carlsson. N. et al., 1995). In this paper we present the main experimental evidence of InP QDs embedded in InGaP matrices grown on GaAs (100) substrates by insertion of GaP layers. QD (or island) densities $\sim 10^9 \text{ cm}^{-2}$ and size distribution and optical properties of InP QDs have been reported. In the theoretical model of the S-K growth mode, QD growth depends both on the strain and the surface condition of the layer upon which the dots are grown. Therefore, the insertion of GaP interface layers between $\text{In}_{0.49}\text{Ga}_{0.51}\text{P}$ matrix and InP QDs layer are also expected to change the morphology, growth characteristics and optical properties of the InP SAQDs.

Experimental Procedure

In this study, quantum dots composed of InP embedded in $\text{In}_{0.49}\text{Ga}_{0.51}\text{P}$ matrix were carried out in a horizontal MOVPE reactor AIXTRON, AIX200/4 with a rotating substrate holder on nominally (001) oriented GaAs substrate. During MOVPE growth, GaAs substrates were placed at the center of the susceptor. For InP QDs on GaAs substrate growth, trimethylgallium (TMGa) and trimethylindium (TMIn), tertiarybutylarsine (TBAs) and tertiarybutylphosphine (TBP) were used as source precursors. Epitaxial growth conditions were a total pressure of 100 mbar, H_2 total flow rate of 13,000 sccm denotes cubic centimeter per

minute at STP, temperature of 610 °C, and V/III ratio of source precursors of 18 for InP. Lattice-matched $\text{In}_{0.49}\text{Ga}_{0.51}\text{P}/\text{GaAs}$ structures are becoming major III-V semiconductor systems because they have lower reactivity with oxygen, and more reduced DX centers and lower interfacial recombination rates compared to $\text{AlGaAs}/\text{GaAs}$ systems.

Schematic representation of the InP QDs structure embedded in InGaP matrix grown on (001) GaAs substrate was depicted in figure 1 120 nm GaAs buffer layers were grown on semi-insulating GaAs (001) substrates at 610 °C. After the growth of GaAs buffer, growth of 150 nm lattice-matched $\text{In}_{0.49}\text{Ga}_{0.51}\text{P}$ layers was followed at the same temperature. In all growth process, the growth temperature was fixed at 610 °C. Then 0 - 4 MLs GaP insertion layer was deposited to improve QDs size uniformity. Finally, the single-layer of self-assembled InP QDs was grown at a growth rate of 0.5 ML/s by depositing 4 ML of InP. For PL measurement, other samples with 50 nm $\text{In}_{0.49}\text{Ga}_{0.51}\text{P}$ cap layers were grown under the same condition. We reported the structural, morphological and optical properties of InP QDs due to insertion of 0 – 4 MLs GaP insertion layers by using atomic force microscopy (AFM) and photoluminescence (PL). Room temperature PL measurement was carried out using the 532 nm line of solid state laser and signal was collected by an InGaAs photo-detector. For low temperature PL measurement, the Ar ion laser and a cooled Ge detector were used and the excitation power was 30 mW. This experimental work was carried out at the Nakano Laboratory, University of Tokyo, Japan.

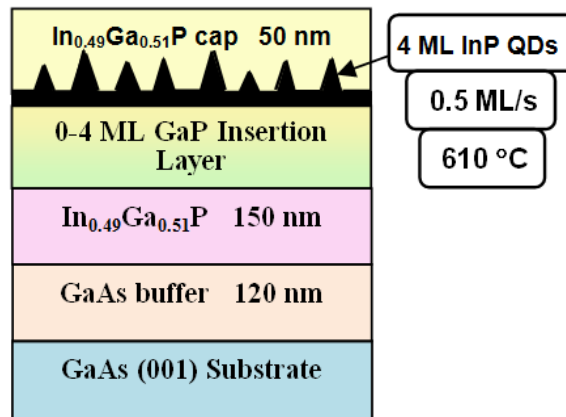


Figure 1 Schematic diagram of the vertical layer structure of InP QDs embedded in InGaP barrier grown on (001) GaAs Substrate.

Results and Discussion

In order to investigate the role of GaP insertion layer on the characterization of size and density of InP SAQDs, we performed the measurement of AFM. Figures 2 (a), (b), (c), (d) and (e) show $1 \times 1 \mu\text{m}^2$ area AFM images of InP quantum dots grown with 0 - 4 ML GaP insertion layer. The study of nanostructure formation and distribution of their size and height for insertion of GaP layer thickness reveals that average height and diameter of smaller (bigger) QDs are 13 nm (28 nm) and 66 nm (87 nm), respectively. The average height and diameter of InP QDs without GaP IL are 25 nm and 85 nm. Both size and height are generally decreased by increasing the thickness of GaP insertion layer. The sample with 2 ML GaP insertion layer shows a significantly improved size, height dispersion and homogeneity. The dot density increases from $2.3 \times 10^9 \text{ cm}^{-2}$ to $4.2 \times 10^9 \text{ cm}^{-2}$ due to insertion of 0 ML - 2 ML GaP layers and then decrease again to $3.3 \times 10^9 \text{ cm}^{-2}$ due to insertion of 3 ML- 4 ML GaP layer.

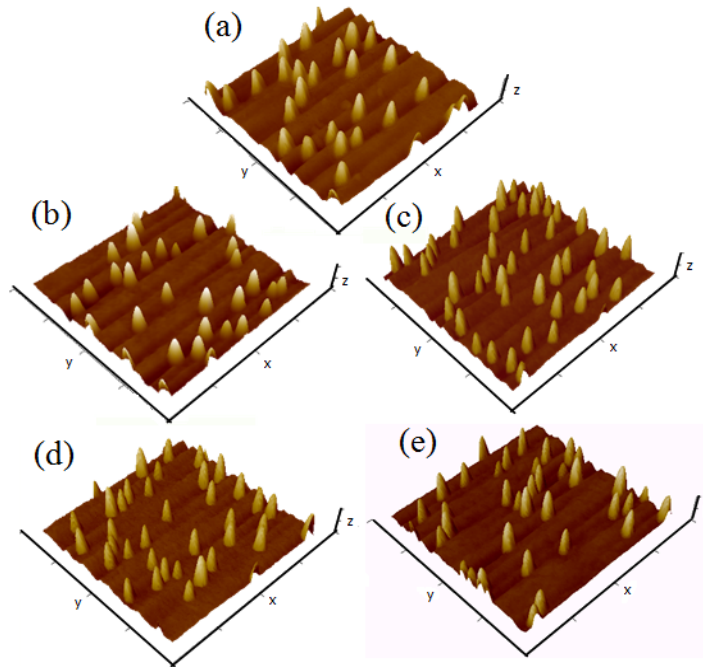


Figure 2 Typical ($1 \times 1 \mu\text{m}^2$) scan range AFM images of InP QDs embedded in InGaP barrier with (a) 0 ML (b) 1 ML (c) 2 ML (d) 3 ML (e) 4 ML GaP layers.

The maximum density of $4.2 \times 10^9 \text{ cm}^{-2}$ and the smallest uniform InP QDs were obtained with 2 ML GaP insertion layer. By the insertion of 2 ML GaP layer, the QDs size was quite increased and density was decreased again. This observation indicated that QDs density first increased with increasing of GaP insertion layer thickness and then it was saturated at 2 ML GaP insertion layer. Such behavior showed the nuclei centers first increased with the increase of GaP insertion layer thickness from 0 ML to 2 ML, afterwards nucleation was completed and further increased in the thickness did not significantly increase the density of QDs. It is likely that the incorporation efficiency of In during the deposition of GaP layer reduces as the strain increases. Another important parameter in the growth of semiconductor III-V quantum dots is the dots density. Figure 3 summarizes the changes in the QDs density and QDs mean height with the GaP insertion layer thickness. Since the growth conditions were the same in all cases, decrease in QDs height, diameter and increase in density with GaP insertion layer indicates that the insertion of thin GaP layer resulted in more material deposition. The dot density increases from $2.3 \times 10^9 \text{ cm}^{-2}$ to $4.2 \times 10^9 \text{ cm}^{-2}$ due to the insertion of 0 ML - 2 ML GaP layers and then decrease again to $3.3 \times 10^9 \text{ cm}^{-2}$ due to insertion of 3 ML- 4 ML GaP layer. The improvement of GaP insertion layer effect on InP QDs can be seen at 2 ML GaP layer.

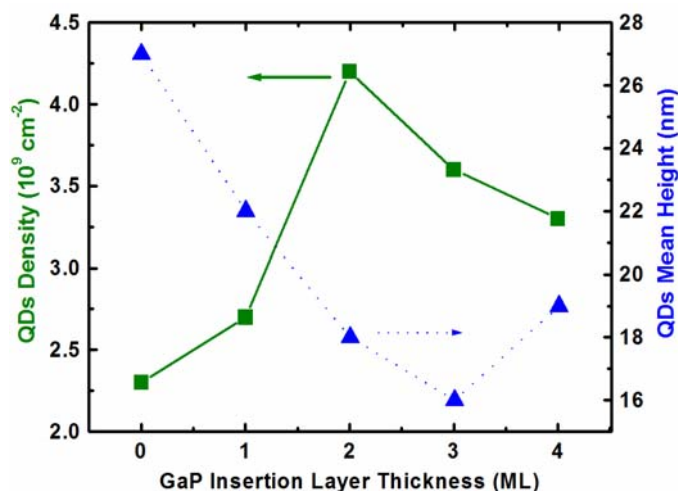


Figure 3 Effect of GaP insertion layer on QDs average size and density for InP SAQDs embedded in InGaP grown at $610 \text{ }^\circ\text{C}$.

Regarding the growth technique, realization of wavelength tunable InP/GaAs QDs by MOVPE is highly desirable, which is the most common growth technique for InP based photonic devices. The evolution of the RT photoluminescence spectra of InP QDs as a function of the thickness of the GaP insertion layer is shown in figure 4. It was found that the InP QDs gave strong photoluminescence (PL), which in fact dominated the spectrum from the samples. The InP QDs without any GaP insertion layer shows PL peak at 814 nm and this InP QDs PL peak is overlapping with GaAs buffer photoluminescence peak. After insertion of 1-4 ML GaP layers, InP QDs photoluminescence peaks were observed separately with GaAs buffer layer photoluminescence peaks. When a 1 ML GaP insertion layer is introduced, the PL intensity decreases and blue-shift noticeably with a peak at 786 nm. As the GaP insertion layer thickness increases from 1 ML to 2 ML, PL intensity increases again and PL peak blue shifts to 781 nm. But the InP QDs with a 3 ML GaP insertion layer show slightly red shifted PL centered at 780 nm and intensity is decreased again. The insertion of 4 ML GaP insertion layer thickness, the PL peak intensity is red-shifted at 783 nm and PL intensity is higher than other GaP insertion layers thickness. The observed blue and red shifts with GaP insertion layer thickness are due to the reduction and increase in the QDs height respectively.

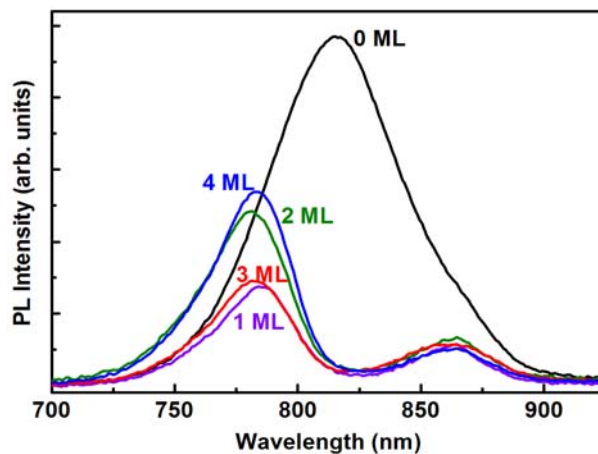


Figure 4 The room temperature PL spectra of the InP QDs grown on the InGaP barrier with 0 – 4 ML thick GaP insertion layer between the InP QDs and the InGaP barrier.

In order to investigate the internal quantum efficiency (QE) and the origin of the emission lines, temperature dependent PL measurements were carried out. Low temperature PL spectra were measured over temperatures range (20 – 250 K) using Ar ion laser, a cooled Ge detector and excitation power was carried out 30 mW. Figure 5 shows series of the PL spectra of InP QDs with 0-4 ML GaP insertion layers under various temperatures. It was observed that the emission spectra at 150, 180 and 250 K temperatures for 0-4 MLs GaP insertion layers samples are very similar in shape. With increasing temperature, the total emission intensity decreases, with various temperatures range, which is presumably due to the interplay between various capture and recombination channels. Indeed, the spectra of GaP insertion layer samples differ in their energy position, in their spectral width and in their relative intensities from the spectra of no GaP insertion layer sample. It was observed at individual temperature, the PL peak was blueshifted and FWHM was reduced by insertion of GaP layers. This result can be understood in terms of the strain-induced interdiffusion between InP and GaP insertion layers, resulting in the size of the quantum dots becoming smaller.

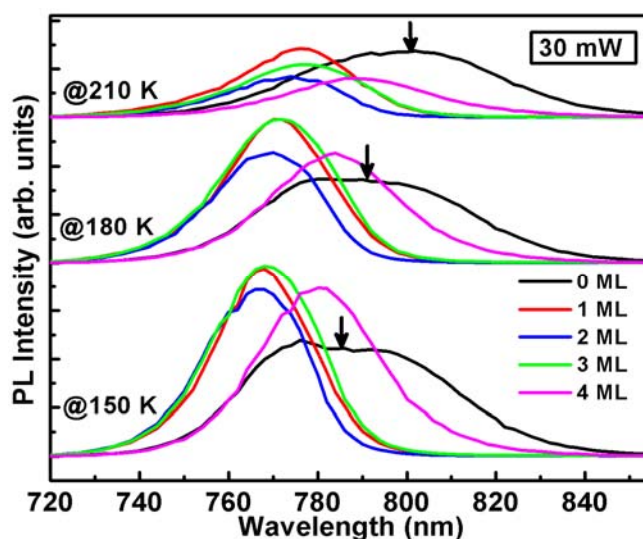


Figure 5 Series of the PL spectra of InP QDs with 0-4 ML GaP insertion layers at temperatures range 150, 180 and 210 K.

Figure 6 displays the temperature dependence of the PL intensity for InP QDs with 0-4 ML GaP insertion layers. The energy position is quite stable in the range of 20-120 K, which can be attributed to very strong localization of exciton in the QDs. However, when the temperature is above 120 K, the drop off the intensity is notably reduced. The results may reflect a reduction of carrier leakage from the QDs. It is clearly observed that insertion of GaP layers can increase luminescence intensity significantly in the temperature range under ~ 150 K. The inset shows the temperature dependence of the PL spectra of InP QDs resulting from 1 ML GaP insertion layer. The PL peak position suffers redshift with increasing temperature. As a result, photogenerated carriers transfers and relax into energetically low-lying states, giving rise to the redshift of the excitation energy as observed in the PL spectra. In case of 2, 3 and 4 ML GaP insertion layer samples, the same trend was observed.

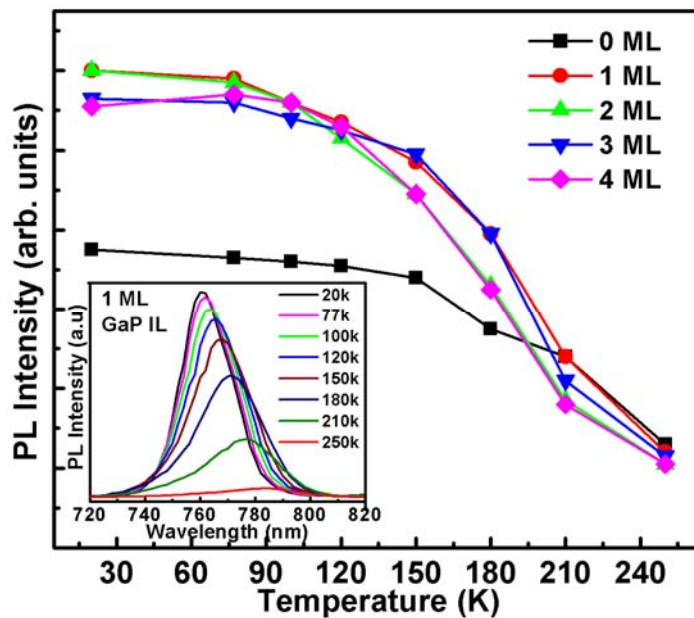


Figure 6 The evolution of the temperature dependence of the PL intensity for InP QDs with 0-4 ML GaP insertion layers. The inset shows the temperature dependence of the PL spectra of InP QDs resulting from 1 ML GaP insertion layer.

The PL emission wavelength as a function of temperature and the thickness of GaP insertion layers is shown in figure 7. The emission wavelength is blue shifted by insertion of GaP layers and it was significantly improved at higher temperatures. The blue shift was significantly observed at 1 and 2 MLs after that the shift was red shifted at 3 and 4 MLs due to the effect of dots size fluctuation. The emission shift can be affected by energy barrier height, stress and strain-induced interdiffusion during the GaP insertion layer growth. The shift is affected not only these factors but also by the QDs size and composition. In addition, the insertion of GaP layer enables to tune the QDs luminescence transition within the 0.76-0.81 μm red spectral range.

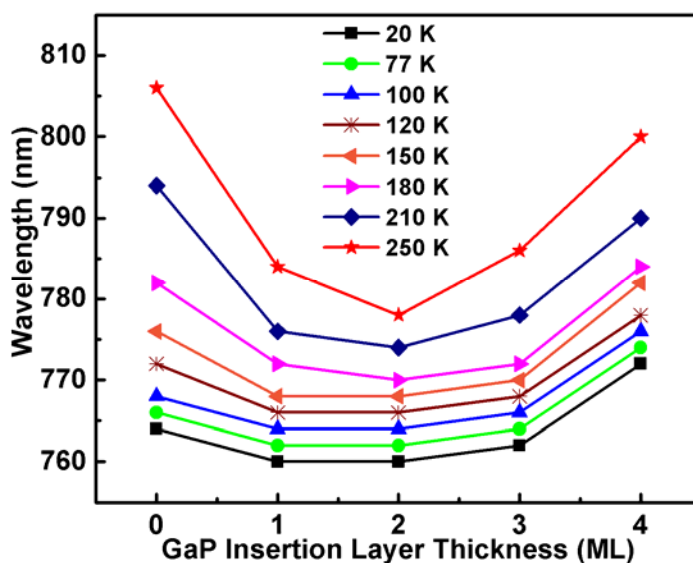


Figure 7 The PL emission wavelength as a function of GaP insertion layers thickness and temperature.

Conclusion

The insertion of 0 - 4 ML GaP layer achieves increase density and it also reduces the size and height of QDs that were the better conditions for InP QDs. The QDs density increment of $2.3 \times 10^9 \text{ cm}^{-2}$ to $4.2 \times 10^9 \text{ cm}^{-2}$ has been achieved at a growth temperature of 610°C with a growth rate of 0.5 ML/s. A thin GaP insertion layer on InP QDs led to a blue-shift of the

RT-PL peak. Insertion of GaP insertion layers leads to smaller dots and the luminescence shifts with GaP insertion layers are due to reduction and increase in QDs size respectively. Measurements of the quantum efficiency of emission from these structures in relation to temperature (20-250 K) demonstrated that the PL spectra are a superposition of InP QDs. The intensity ratio of emissions depends on temperature, with the wavelength varying within 0.76-0.82 μm . Thus, the obtained InP growth structure can be used to create radiation sources readily tunable in the red spectral range by varying GaP insertion layer thickness.

Acknowledgements

The authors wish to thank ASEAN University Network/Southeast Asia Engineering Education Development Network (AUN/SEED-Net), Chulalongkorn University and University of Tokyo for the support of this work. The authors also would like to appreciate Dr Win Win Thar, Professor and Head of the Department of Physics, University of Yangon for her kind permission to carry out this work.

References

- Carlsson, N., Georgsson, K., Montelius, L., Samuelson, L., Seifert, W. & Wallenberg, R. (1995) *J. Cryst. Growth* **156**, 23 - 27.
- DenBaars, S.P., Reaves, C.M., Bressler-Hill, V., Varma, S., Weinberg, W.H., & Petroff, P.M., (1994) *J. Cryst. Growth* **145**, 721- 725.
- Leonard, D., Pond, K. & Petroff, P.M., (1994) *Phys. Rev. B* **50**, 11687 - 11690.
- Ribeiro, E., Maltez, R. L., Carvalho, W. Jr., Ugarte, D., & Medeiros-Ribeiro, G., (2002) *Appl.Phys. Lett.* **81**, 2953-2957.
- Richter, D., Robbach, R., Schulz, W.-M., Koroknay, E., Kessler, C., Jetter, M., & Michler, P., (2010) *Appl.Phys.Lett.* **97**, 63107 - 63110.
- Ren, H.-W., Nishi, K., Sugou, S., Sugisaki, M. & Masumoto, Y., (1997) *Jpn. J. Appl. Phys.* **36**, 4118 -4121.
- Thompson, A. G., Stall, R. A., Kroll, W., Armour, E., Beckham, C., Zawadzki, P., Aina, L. & Siepel, K., (1997) *J. Cryst. Growth* **170**, 92 - 96.
- Zwiller, V., Blom, H., Jonsson, P., Panev, N., Jeppesen, S., Tsegaye, T., Goobar, E., Pistol, M., Samuelson, L. & Björk, G., (2001) *Appl.Phys.Lett.* **78**, 2476 - 2479.